

Initial Stages of Pattern Formation in Rayleigh-Bénard Convection

Christopher W. Meyer, Guenter Ahlers, and David S. Cannell

Department of Physics, University of California, Santa Barbara, California 93106

(Received 15 June 1987)

Flow-visualization studies and heat-flux measurements during the early evolution of convection in a cylindrical container of aspect ratio 10 (radius/height) are reported. The heat current was ramped linearly, or modulated time periodically, from below to above the onset value. A novel sidewall design allowed pattern formation to occur independently of container geometry. In the earliest stages, the patterns were composed of irregularly arranged cells and varied randomly between experimental runs. The results demonstrate the importance of stochastic effects during the pattern evolution.

PACS numbers: 47.20.Bp, 47.25.Qv

Pattern formation in nonequilibrium systems has received considerable attention recently.¹ An important question is whether these patterns emerge in a purely deterministic manner or whether noise plays a central role in their formation.^{2,3} An interesting example in which stochastic effects seem important is a recent study of dendritic growth.⁴ Rayleigh-Bénard convection in a horizontal fluid layer subjected to a vertical temperature gradient is particularly well adapted for the study of such processes because the equations of motion are well established, and the boundary conditions are simple and can be controlled well. Indeed, fluctuations near the convective threshold have received considerable theoretical attention,² but so far there has been no convincing experimental evidence of their importance. Stability analysis shows that the *steady-state* pattern near threshold should consist of straight parallel rolls for the laterally infinite system. Experimentally we find that the *initial* state of pattern formation is usually dominated by transient horizontal thermal gradients associated with the sidewalls,^{3,5,6} which result in patterns reflecting the symmetry of these lateral boundaries. We have eliminated this forcing, enabling us to observe patterns which should be representative of what would be seen in a laterally infinite system. These patterns, *when they first emerge*, consist of randomly positioned cellular flow, which is irreproducible from one experimental run to the next. The irreproducibility implies that stochastic perturbations play a crucial role in the initial stages of pattern formation when deterministic effects (such as horizontal gradients) are reduced to sufficiently low levels.

The working fluid was water at 25.5°C. We used two types of sidewalls for a cylindrical container of inner diameter 6.35 cm and height $d=0.318$ cm. The first forced flows which reflected the sidewall geometry. It consisted of a ring of high-density polyethylene of thermal diffusivity $\kappa \approx 2.2 \times 10^{-3}$ cm²/s, which differs from that of water (1.47×10^{-3} cm²/s). This mismatch resulted in horizontal temperature differences between the fluid and the wall, during the period while the vertical temperature difference was being changed, which

were sufficient to control the pattern evolution.^{3,5} The second sidewall did not force any flows. It consisted of a polyethylene ring similar to that described above, except that it had an inner diameter of 7.6 cm, and the region between its inner surface and the fluid was occupied by an annulus of 5% polyacrylamide gel which has thermal properties very close to those of water. The remainder of the apparatus was as described previously.⁶

A first experiment involved ramping the heat current j linearly through the convective threshold,³ with dimensionless ramp rate β such that $j = j_0 + \beta t$. We measured j in units of the critical current for the onset of convection with steady heating and t in units of the vertical thermal diffusion time $t_v = d^2/\kappa$. Our ramp rates were in the range $0.01 \leq \beta \leq 0.30$. All values of β gave qualitatively similar results. After an initial transient, the temperature difference ΔT increased linearly with time until convection began. We defined $t=0$ to be the point where $\Delta T = \Delta T_c$, and j_0 to be the current at $t=0$. The convective heat current j^{conv} was determined as described elsewhere.³

As in Ref. 3, one attempt to distinguish between stochastic and deterministic effects consisted of comparing the data for j^{conv} with the predictions of a Landau amplitude equation

$$\tau_0 \dot{A} = \epsilon A - g A^3 + k A^5 + f. \quad (1)$$

Here $\epsilon(t) \equiv \Delta T(t)/\Delta T_c - 1$, g and k are constants found from independent static heat-flux measurements, τ_0 is obtained from a linear stability analysis,⁷ and $j^{\text{conv}} = A^2$. First, a constant phenomenological field f was used as the only adjustable parameter in the model. Equation (1) was integrated with initial conditions $\epsilon = -\beta$ and $A = f/\beta$, and f was least-squares adjusted to fit the data. Next, we also compared j^{conv} with the predictions of a stochastic equation,³ where the field f of Eq. (1) was taken as a Gaussian noise term with $\langle f(t)f(t') \rangle = 2\tau_0 F \delta(t-t')$. The approximate solution of Eq. (1) given in Ref. 3 was fitted to the data by adjusting F .

The first two figures illustrate the difference between forcing and nonforcing sidewalls. The time-dependent

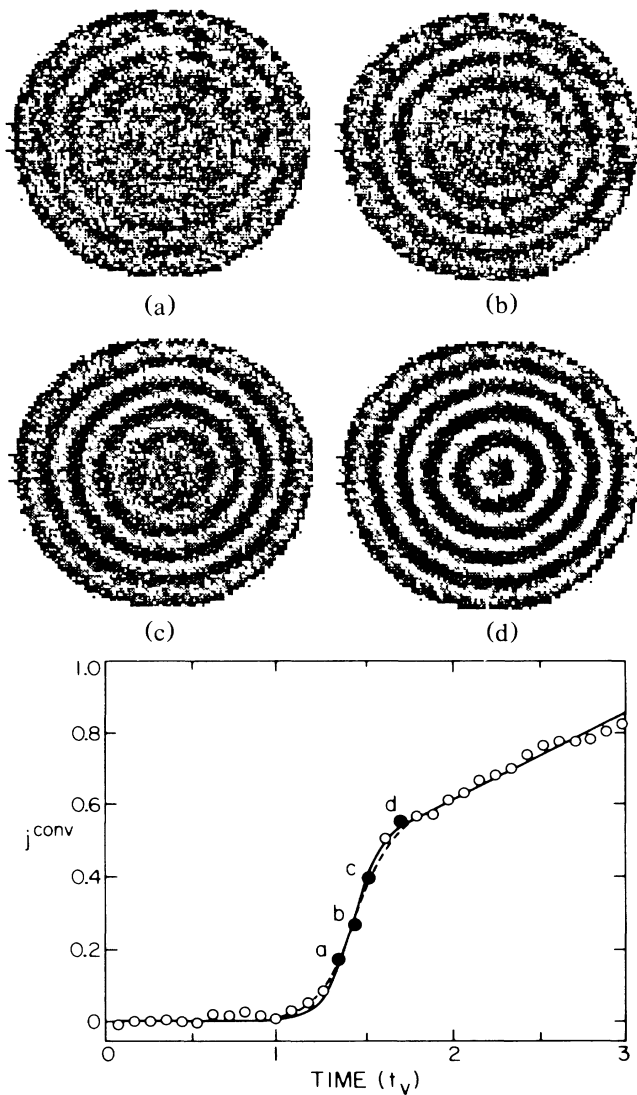


FIG. 1. Shadowgraph images of the emerging pattern and data for the convective heat flux j^{conv} , as a function of time, resulting from a linear heat current ramp, with a dimensionless ramp rate $\beta=0.27$, for a cell with polyethylene sidewalls. Time is given in units of the vertical thermal diffusion time, and j^{conv} is in units of the heat flux at the onset of convection for steady heating. Solid circles correspond to the points where images were taken.

convective heat current is shown below the images, with solid circles corresponding to the times at which the images were taken. Figure 1 shows the results for the forcing sidewalls. The pattern clearly reflects the geometry of the walls, and the images illustrate how this pattern spreads. It develops in the region adjacent to the wall and moves inward filling the cell. The solid curve in the plot is given by the deterministic equation with $f=2.70 \times 10^{-4}$, and the dashed curve is the solution to the stochastic equation with $F=2.74 \times 10^{-6}$. Both

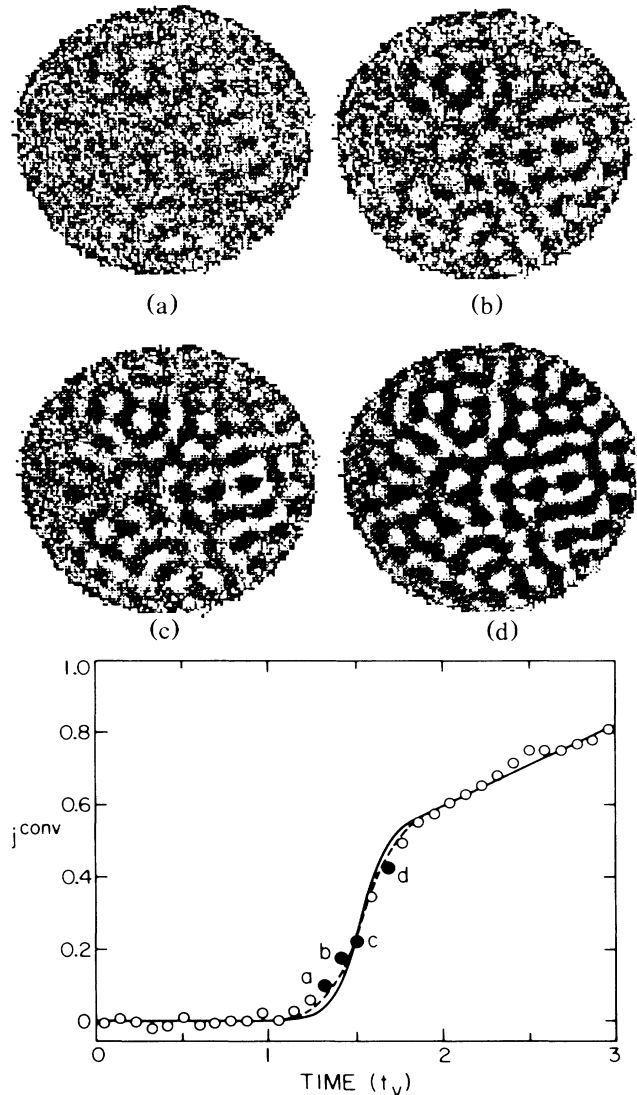


FIG. 2. Images and convective-heat-flux data as in Fig. 1 for the same ramp rate, but for a cell with sidewalls made of 5% polyacrylamide gel.

theoretical curves are in good agreement with the data, and this comparison thus cannot distinguish between a deterministic and a stochastic forcing field.

The results obtained with the nonforcing sidewalls are shown in Fig. 2. In this case the pattern was not influenced by the walls. It emerged at the same time throughout the cell, and its form was not correlated with the container geometry. Interestingly, the pattern is not composed of rolls, but rather of irregularly arranged cells with no clear geometrical structure.⁸ Similar patterns were also obtained in a cell with square sidewalls. The best-fit field values were $f=1.28 \times 10^{-4}$ and $F=6.03 \times 10^{-7}$, for the circular cell. The smaller values for the fields compared to the case illustrated in Fig. 1

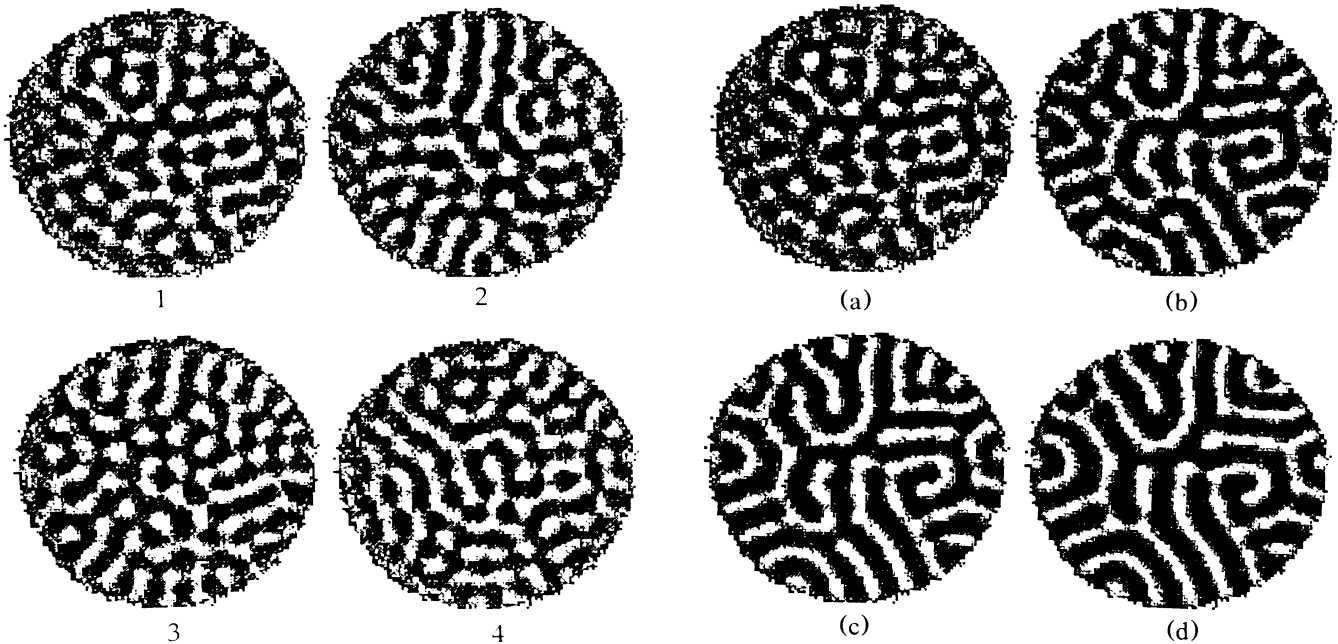


FIG. 3. Emerging patterns for consecutive experimental runs, all with ramp rate $\beta=0.27$, for the cell with gel sidewalls. The images were taken at the time corresponding to point d in Fig. 2, and clearly show that the emerging pattern is not reproducible.

demonstrate the weaker forcing of the gel walls relative to the plastic walls. Although the stochastic equation provides a slightly better fit in this case, the data for j^{conv} cannot distinguish convincingly between the deterministic and the stochastic field.³ However, one might hope that a detailed theory of the stochastic forcing, when it becomes available, will yield a value for F to be compared with the measurement.⁹

The patterns emerging from thermal ramps with the polyethylene walls were always reproducible. Those arising from ramps with the gel walls were qualitatively similar, but differed in successive runs. This is illustrated in Fig. 3, which shows images (at the time corresponding to point d in Fig. 2) for four consecutive runs, all with $\beta=0.27$. The cells of the flow were located in different places each time, causing no two patterns to be the same. This pattern irreproducibility implies that the cellular pattern was induced by a stochastic perturbation.

The cellular patterns which formed during the ramps healed into a roll-like pattern within a few thermal diffusion times. This evolution is illustrated in Fig. 4, where we show later images of the ramp of Fig. 2.

In a second set of experiments, we observed random cellular flow involving pattern decay and reformation as a stationary process.¹⁰ Here the heat current j was modulated sinusoidally, resulting in $\epsilon(t) = \epsilon_0 + \delta \sin(\Omega t)$

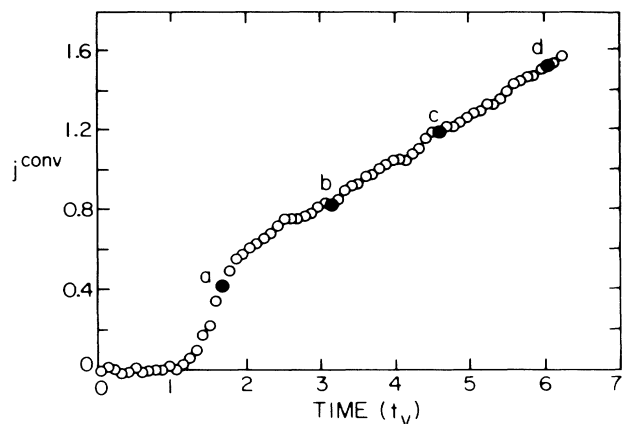


FIG. 4. Evolution of the pattern of Fig. 2, under continued ramping, showing healing leading to a roll-like structure. Heat-flux data are also shown, with point a corresponding to point d of Fig. 2.

+ (higher harmonics). When ϵ_0 was sufficiently large, an initially induced roll pattern persisted, periodically fading away and then reappearing unchanged. For lower ϵ_0 , however, the amplitude of the convection decreased to a small enough value so that perturbations could influence the pattern, and the reemerging structure, after many cycles, consisted of random cells, qualitatively the same as those shown in Fig. 2. Figure 5 shows as solid circles the experimentally determined boundary in the ϵ_0 - δ plane below which cellular flow was seen for $\Omega = 1$. The solid curve was obtained by postulating that the roll pattern would disintegrate and cellular flow would emerge if the minimum of $j^{conv}(t)$ during one cycle fell below a critical value taken to be 1.25×10^{-6} .¹¹ It is in-

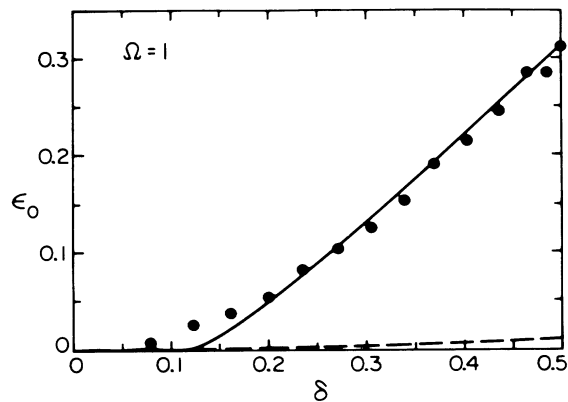


FIG. 5. Data for the boundary above which the reemerging pattern in successive cycles of modulation was reproducible and roll-like, and below which it was cellular. The solid curve was obtained by assuming pattern reproducibility for $j^{\text{conv}}(t) \geq 1.25 \times 10^{-6}$ throughout each cycle. The dashed curve shows the convective threshold shift predicted from a Lorenz model (Ref. 11).

interesting to note that such a small value of j^{conv} would be reached under steady driving only for $\epsilon \approx 10^{-6}$, and that fluctuations are predicted² to play an important role for such a small value of ϵ .

The dashed curve in Fig. 5 shows the convective threshold shift $\epsilon_c(\Omega, \delta)$ predicted by a Lorenz model,¹¹ which assumes that a roll pattern may remain intact down to arbitrarily low values of j^{conv} . Clearly this model is not applicable for the parameters of Fig. 5 where noise plays a dominant role in inducing convection. At higher modulation frequencies, where j^{conv} does not have time to decay below 10^{-6} , the cellular flow should not occur, and the predictions for ϵ_c of the Lorenz model should be observable.

We would like to stress that the cellular structures seen in our modulation experiments are not the hexagons that have been predicted¹² to be stable for certain modulation parameters. The irreproducibility and irregularity of the patterns should make this conclusive.

We are grateful to Giovanni Dietler and Roger Drake for their help in preparing our gels. This work was supported by National Science Foundation Grant No. MSM-85-14917 and U.S. Department of Energy Grant No. DE-FG03-87ER13738.

¹For instance, see *Spacio-Temporal Coherence and Chaos in Physical Systems*, edited by A. R. Bishop, G. Grüner, and B. Nicolaenko (North-Holland, Amsterdam, 1986).

²V. M. Zaitsev and M. I. Shliomis, *Zh. Eksp. Teor. Fiz.* **59**, 1583 (1970) [*Sov. Phys. JETP* **32**, 866 (1971)]; R. Graham, *Phys. Rev. A* **10**, 1762 (1974); J. Swift and P. C. Hohenberg, *Phys. Rev. A* **15**, 319 (1977).

³G. Ahlers, M. C. Cross, P. C. Hohenberg, and S. Safran, *J. Fluid Mech.* **110**, 297 (1981).

⁴A. Dougherty, P. H. Kaplan, and J. P. Gollub, *Phys. Rev. Lett.* **58**, 1652 (1987).

⁵M. C. Cross, P. C. Hohenberg, and M. Lücke, *J. Fluid Mech.* **136**, 269 (1983).

⁶V. Steinberg, G. Ahlers, and D. S. Cannell, *Phys. Scr.* **32**, 534 (1985).

⁷R. Behringer and G. Ahlers, *Phys. Lett.* **62A**, 329 (1977); M. A. Dominguez-Lerma, G. Ahlers, and D. S. Cannell, *Phys. Fluids* **27**, 856 (1984).

⁸Similar cellular flow has been observed in computer simulations of the evolution of convection from random initial conditions [H. S. Greenside and W. M. Coughran, Jr., *Phys. Rev. A* **30**, 398 (1984)].

⁹The value of F from the ramp experiment has already been used by J. Swift and P. C. Hohenberg (unpublished) to reproduce the modulation results given in Fig. 5.

¹⁰A different nonforcing sidewall design, involving a thin horizontally projecting fin at the midplane of the cell, was used in these runs.

¹¹For this calculation we used the Lorenz model [E. N. Lorenz, *J. Atmos. Sci.* **20**, 130 (1963)] of G. Ahlers, P. C. Hohenberg, and M. Lücke, *Phys. Rev. A* **32**, 3493, 3519 (1985).

¹²M. N. Roppo, S. H. Davis, and S. Rosenblat, *Phys. Fluids* **27**, 796 (1984); P. C. Hohenberg and J. Swift, *Phys. Rev. A* **35** 3855 (1987).